Dolphins First: Dolphin-Aware Communications in Multi-Hop Underwater Cognitive Acoustic Networks

Xuanheng Li, *Student Member, IEEE*, Yi Sun, *Member, IEEE*, Yuanxiong Guo, *Member, IEEE*, Xin Fu, *Member, IEEE*, and Miao Pan, *Member, IEEE*

***Abstract*— Acoustic communication is the most versatile and widely used technology for underwater wireless networks. However, the frequencies used by current acoustic modems are heavily overlapped with the cetacean communication frequencies, where the man-made noise of underwater acoustic communications may have harmful or even fatal impact on those lovely marine mammals, e.g., dolphins. To pursue the environmental friendly design for sustainable underwater monitoring and exploration, specifically, to avoid the man-made interference to dolphins, in this paper, we propose a cognitive acoustic transmission scheme, called dolphin-aware data transmission (DAD-Tx), in multi-hop underwater acoustic networks. Different from the collaborative sensing approach and the simplified modeling of dolphins' activities in existing literature, we employ a probabilistic method to capture the stochastic characteristics of dolphins' communications, and mathematically describe the dolphin-aware constraint. Under dolphin-awareness and wireless acoustic transmission constraints, we further formulate the DAD-Tx optimization problem aiming to maximize the end-to-end throughput. Since the formulated problem contains probabilistic constraint and is NP-hard, we leverage Bernstein approximation and develop a three-phase solution procedure with heuristic algorithms for feasible solutions. Simulation results show the effectiveness of the proposed scheme in terms of both network performance and dolphin awareness.**

***Index Terms*— Underwater cognitive acoustic communications, multi-hop transmission, network optimization, Bernstein approximation, mix-integer non-linear programming.**

I. Introduction

MORE than 70% of this planet's surface covered by water, numerous resources underneath, and almost 95% of underwater world less explored makes the research of underwater communications and networks mysterious and attractive. Since electromagnetic waves attenuate significantly in the conductive water medium, and optical waves have severe scattering effect and thus limited transmission range, acoustic signals become the best option for underwater wireless communications [1], [2]. The corresponding underwater acoustic networks (UANs) has a wide range of applications, such as underwater environment monitoring, underwater resource exploration, offshore infrastructure protection, target tracking, and oceanography data collection [3]. Despite the various application scenarios, underwater acoustic communications (UACs) still suffer from many issues, such as long propagation delay, time-varying acoustic channels, high channel error rates and limited spectrum frequencies, etc., which have raised many outstanding research works endeavoring to address them and improve the network performance [4]–[6].

Besides the communication quality issues, it is noteworthy that the man-made UAN may not be the only acoustic system in its deployed area, where multiple natural acoustic systems like marine mammals might appear in the same area using sounds for communications, echolocation and foraging as well [7]. Since the frequencies used by current acoustic modems are heavily overlapped with the marine mammals' communication frequencies (e.g., most UANs operate on mid-frequencies from 1 kHz to 40 kHz, and the bottlenose dolphin sends whistle communication signals from 200 Hz to 24 kHz and click echolocation signals from 200 Hz to 150 kHz, respectively) [8], [9], the man-made noise of UANs will have harmful or even fatal impact on those lovely animals [8]–[12].[1] Therefore, minimizing the harmful interference to marine mammals, meanwhile maintaining high network performance is significant.

Aiming at environment friendly UACs for sustainable underwater monitoring and exploration, some pioneering works have proposed underwater cognitive acoustic networks (UCANs) as a promising solution [8]–[12]. In [8], Wang *et al.* introduced the concept of UCANs, in which certain oper-

Manuscript received March 8, 2016; revised July 16, 2016; accepted October 16, 2016. Date of publication November 1, 2016; date of current version April 7, 2017. The work of X. Li was supported by the China Scholarship Council. The work of X. Fu was supported in part by NSF under Grant CCF-1619243, Grant CCF-1537085 (CAREER), and Grant CCF-1537062. The work of M. Pan was supported by the U.S. National Science Foundation under Grant CNS-1343361, Grant CNS-1350230 (CAREER), and Grant CPS-1646607. The associate editor coordinating the review of this paper and approving it for publication was Z. Wang.

X. Li and Y. Sun are with the School of Information and Communication Engineering, Dalian University of Technology, Dalian 116024, China (e-mail: lixuanheng@mail.dlut.edu.cn; lslwf@dlut.edu.cn).

Y. Guo is with the School of Electrical and Computer Engineering, Oklahoma State University, Stillwater, OK 74078 USA (e-mail: richard.guo@okstate.edu).

X. Fu and M. Pan are with the Department of Electrical and Computer Engineering, University of Houston, Houston, TX 77204 USA (e-mail: xfu8@central.uh.edu; mpan2@uh.edu).

Color versions of one or more of the figures in this paper are available online at http://ieeexplore.ieee.org.

Digital Object Identifier 10.1109/TWC.2016.2623604

[1] Dolphins are heavily dependent on sound for food-finding, communication, reproduction, and navigation, and thus really sensitive to the anthropogenic noise imposed in their living environment. Some serious consequences may occur if they are exposed into a noisy environment for a long period of time, such as changes in diving and foraging behavior, displacement from critical feeding and breeding grounds, temporary and permanent hearing loss, etc [13], [14].

ating settings (i.e., transmitting power, carrier frequency, modulation, etc.) can be adjusted adaptively in real-time based on the surrounding environment, presented the potential network structure and applications of UCANs, and outlined the future development of UCANs. In [9], [10], Luo *et al.* identified the research challenges and opportunities of the UCAN designs due to the unique underwater features and environmental friendly requirements. To tackle those challenges, Cheng *et al.* in [12] proposed a framework of acoustic channel availability prediction to protect marine mammals against man-made interferences, in which a simplified activity model is employed for different types of marine mammals and the probability of the occurrence of marine mammals' communications is assumed to be a priori knowledge. Inspired by the research in cognitive radio networks (CRNs) [15], [16], Luo *et al.* in [11] proposed a receiver-initiated spectrum management (RISM) system for UCANs, which regards marine mammals as primary users and acoustic modems/sensors as secondary users. To avoid harmful interferences to marine mammals, RISM allows acoustic sensors to conduct collaborative spectrum sensing and choose the channel based on the sensing results.

However, different from the terrestrial CRNs, UCANs may not be able to afford the overhead incurred by collaborative sensing of marine animals. Generally speaking, collaborative sensing requires a frequent sensing information exchange among participating nodes. While the time and energy cost on those control packet transmissions carried by electromagnetic waves might be a minor issue in CRNs, it cannot be ignored in the underwater environment when taking the long preamble and propagation delay of acoustic communications into account [6]. The increased overhead burden by frequent sensing information exchange might even block the data transmission in UCANs. In addition, most existing works [10]–[12] assume a simple communication/activity model for different species of marine mammals (i.e., seals, whales, dolphins, porpoises, manatees, etc.). In fact, different species of marine mammals have different patterns of communications/behaviors. It might be very difficult, if not impossible, to find an universal communication/activity model for all kinds of marine mammals.

Underlay based power management is a common approach in terrestrial CRNs to realize the spectrum sharing between primary users (PUs) and secondary users (SUs) [17], [18]. Through specific schemes, the interference caused by SUs at a primary receiver is limited below certain level (interference temperature constraint), meanwhile optimizing certain performance metric, such as minimizing the power consumption of SUs [19], maximizing the transmission rate of SUs [20], etc. Inspired by these works, owing to the development on soft-ware defined acoustic modems [21], [22], to address the issues above, we propose a dolphin-aware data transmission (DAD-Tx) scheme in multi-hop underwater cognitive acoustic networks (MUCANs), which targets at (i) protecting a typical species of marine mammals, dolphins, against the interference of UACs, i.e., control the power of each transmitting node by treating dolphins as PUs, and (ii) improving the end-to-end throughput by elaborately scheduling the network resource. Specifically, based on field records of dolphins' activities [23], we define a dolphin-active distance [2] for each underwater acoustic modem, and mathematically describe the dolphin-awareness as a probabilistic constraint to control the modems' transmission power. Under the dolphin-aware constraint and multiple acoustic transmission constraints, we formulate the optimal DAD-Tx problem with the objective of maximizing the end-to-end throughput in MUCANs, and develop algorithms for feasible solutions. Note that the proposed DAD-Tx scheme can easily be extended to protect other species of marine mammals as long as the statistics/records of their activities in designated area can be provided. Our salient contributions are listed as follows.

- Inspired by the uncertain spectrum supply in CRNs [24], we propose a novel statistics based method to model dolphins' activities in MUCANs. Based on the proposed modeling, we further mathematically describe the dolphin-awareness with a probabilistic constraint.
- With a joint consideration of dolphin-awareness and acoustic transmission features including interference mitigation and flow routing, we formulate the DAD-Tx as an optimization problem, which is a probabilistic constrained optimization without classical solutions.
- To solve the formulated problem, we leverage the Bernstein approximation approach [25] to derive a tractable conservative approximation to the probabilistic constraint of dolphin-awareness. Then, by using the tractable approximation constraint, we convert the stochastic DAD-Tx optimization into a mix-integer non-linear programming (MINLP) problem.
- Since the formulated MINLP problem is NP-hard to solve, we develop a three-phase solution procedure for feasible solutions. Briefly, we first convert the original MINLP problem into a relaxed mix-integer linear programming (R-MILP) problem through convex hull based linear relaxation. Then, we propose a heuristic relax-and-fix based iterative (HRFI) algorithm to determine all integer variables through iteratively solving a sequence of linear programming (LP) problems. Finally, with the fixed integer variables, other variables can be determined by solving two LP problems.

The rest of the paper is organized as follows. We introduce the network model of MUCANs in Section II. In Section III, we propose the DAD-Tx scheme and formulate the optimal DAD-Tx problem under multiple constraints. We derive tractable approximation for the probabilistic constraint and conduct the conversion of the optimization in Section IV. In Section V, we develop a three-phase solution procedure for feasible solutions. Finally, we analyze the simulation results in Section VI and draw conclusion remarks and future works in Section VII.

[2]Dolphins are one of most well-studied marine mammals. Although the explicit behavior of dolphins is still hard to find due to the complex correlations and dynamic physical parameters, some approximate characteristics, e.g., the average dolphin-active distance introduced in the next section, can be obtained by using autonomous acoustic recorders [23].

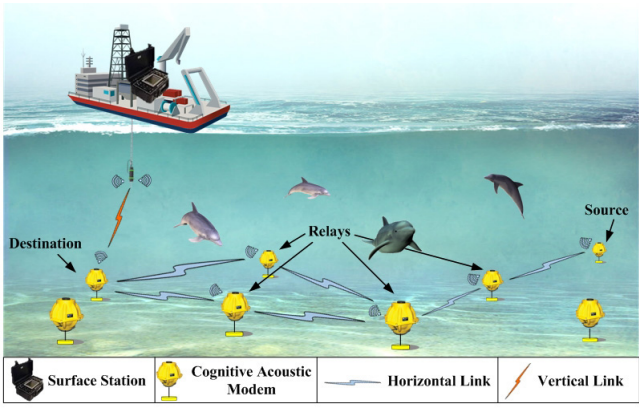

Fig. 1. System architecture of MUCANs.

II. Network Model

A. Network Configuration

We consider a MUCAN consisting of a surface station (SS), a group of cognitive acoustic modems (CAMs) and several dolphins playing around. The CAMs are anchored to the ocean floor for earthquake detection, pollution monitoring or oceanography data collection, and they are interconnected by wireless acoustic links as shown in Fig. 1. The SS plays the role of collecting the sensed information from CAMs and guiding the CAMs' data transmission in a multi-hop manner with joint consideration of power control based dolphin-awareness, interference mitigation and flow routing.

Intuitively, dolphin-aware transmission can be realized by collaboratively sensing dolphins' activities around the CAMs [11]. However, to guide such dolphin-aware multi-hop transmission from the source CAM to the destination CAM, the broadcasting based guidance will be needed frequently, which can cause too much overhead and is troublesome in MUCANs. Therefore, instead of real-time collaborative sensing of dolphins, we achieve the awareness of dolphins based on the statistics of dolphins' activities considering the fact that their habit is closely related to the physical environment with certain characteristics. Since the locations of CAMs are relatively fixed (they are anchored to the ocean floor), the statistics of surrounding dolphins' activities will not have a sudden change within a relatively short period (e.g., several hours, or several days) [23]. So, the transmission guidance is generally needed only once (i.e., for the first time of the establishment of the transmission routes) in such a static underwater sensor network. Furthermore, several promising schemes developed for the reliable control message broadcasting can be adopted to realize the centralized dolphin-aware transmission scheme [26], [27].

B. Modeling of Underwater Acoustic Communications

In this subsection, we present some classical models employed in this paper. For simplicity, we omitted the detailed introduction of them, which can be found in many existing research works [28], [29].

1) Transmission Loss: The transmission loss $L(d, f)$ following the Urick's model in dB for a signal at frequency f (kHz) over a transmission distance d (km) is

$$10\log L(d, f) = k \cdot 10\log\left(d \times 10^3\right) + d \cdot \alpha(f) + A \quad (1)$$

where k is a spreading factor, $\alpha(f)$ is an absorption coefficient, and A is a constant in dB called transmission anomaly representing other factors. For theoretical study, k can be set to 1.5, the absorption coefficient $\alpha(f)$ (dB/km) can be approximated by Thorp's formula as

$$\alpha(f) = \frac{0.11 f^2}{f^2+1} + \frac{44 f^2}{f^2+4100} + 2.75 \times 10^{-4} f^2 + 0.003, \quad (2)$$

and the constant A is neglected in this paper for simplicity as some other works [30], [31].

2) Transmission Range and Interference Range: Suppose that there are $\mathcal{M} = \{1, \cdots, M\}$ available OFDM sub-channels in the MUCAN [32], [33], which are centered at $\{f_1, \cdots, f_M\}$ with bandwidth $\{\Delta f_1, \cdots, \Delta f_M\}$, respectively. Assume that the transmission power at the i-th CAM on sub-channel m is p_i^m. Obviously, the transmission loss is monotonically increasing with the distance and the remaining power after a distance d from the i-th CAM can be expressed approximatively as $p_i^m \cdot L(d, f_m)^{-1}$ due to the narrow bandwidth. Based on a receiving power threshold $P_{\text{CAM}}^{\text{T}}$, we define a transmission range for each CAM i, $\forall i \in \mathcal{N}$, when it transmits on sub-channel m with the power p_i^m as

$$R_{i,m}^{\text{T}} = \arg\max_d \left\{ p_i^m \cdot L(d, f_m)^{-1} \geq P_{\text{CAM}}^{\text{T}} \right\}. \quad (3)$$

Similarly, for the receiving interference, we also set a receiving power threshold as its negligible level, which is denoted as $P_{\text{CAM}}^{\text{I}}$. Then, for CAM i transmitting on sub-channel m, the interference range can be denoted as

$$R_{i,m}^{\text{I}} = \arg\min_d \left\{ p_i^m \cdot L(d, f_m)^{-1} \leq P_{\text{CAM}}^{\text{I}} \right\}. \quad (4)$$

For CAM $i \in \mathcal{N}$, $R_{i,m}^{\text{T}} < R_{i,m}^{\text{I}}$ because $P_{\text{CAM}}^{\text{T}} > P_{\text{CAM}}^{\text{I}}$.

3) Link Capacity: The noise power spectral density (PSD) is usually denoted as the sum of four contributions, i.e.,

$$N(f) = N_t(f) + N_s(f) + N_w(f) + N_{th}(f), \quad (5)$$

which includes turbulence, shipping, wind and thermal noise, respectively. They can be modeled with frequency f(kHz) in dB re μPa per Hz as follows [28]:

$$\begin{aligned} \widehat{N}_t(f) &= 17 - 30\log(f) \\ \widehat{N}_s(f) &= 20s - 60 + 26\log(f) - 60\log(f + 0.03) \\ \widehat{N}_w(f) &= 50 + 7.5w^{1/2} + 20\log(f) - 40\log(f + 0.4) \\ \widehat{N}_{th}(f) &= -15 + 20\log(f), \end{aligned} \quad (6)$$

where $\widehat{N}_x(f) = 10\log N_x(f)$, $x \in \{t, s, w, th\}$. In $\widehat{N}_s(f)$, s indicates the shipping activities on the surface, whose value ranges from 0 to 1 representing low and high activity, respectively, and in $\widehat{N}_w(f)$, w denotes the wind speed in m/s.

TABLE I
THE LIST OF NOTATIONS

Symbol	Definition
$\mathcal{N}$	Set of CAMs in the MUCAN
$\mathcal{M}$	Set of available OFDM sub-channels
$L(d, f)$	Transmission loss at frequency f over a distance d
$\alpha(f)$	Absorption coefficient at frequency f
$P_{\mathrm{CAM}}^{\mathrm{I}}$	Upper bound of the negligible interference power
$P_{\mathrm{CAM}}^{\mathrm{T}}$	Lower bound of the received power for a successful transmission
p_i^m	Transmission power at CAM i on sub-channel m
$R_{i,m}^{\mathrm{T}}$,$R_{i,m}^{\mathrm{I}}$	Transmission/interference range of CAM i on sub-channel m
$R_{i,m}^{\mathrm{Tmax}}$,$R_{i,m}^{\mathrm{Imax}}$	Maximal transmission/interference range of CAM i on sub-channel m using full transmission power
$N(f)$	Noise power spectral density
Δf_m	Bandwidth of the m-th sub-channel
c_{ij}^m	Link capacity from CAM i to CAM j on sub-channel m
$\hat{d}_i$	Dolphin-active distance of CAM i
x_{ij}^m	Binary indicator to mark whether or not sub-channel m is allocated on link CAM i to CAM j
$\mathcal{T}_i^m$	The m-th transmission neighbor set of CAM i
$\mathcal{I}_j^m$	The m-th interference neighbor set of CAM j
$\hat{p}_{ij}^m$	Transmission power of CAM i used for the transmission from CAM i to CAM j on sub-channel m
$P_i^{\max}$	Maximal transmission power of CAM i
f_{ij}	Data flow rate on link from CAM i to CAM j
α	Confidence level in original probabilistic constraint
$P_{\mathrm{Dol}}^{i,m}$	Dolphin-sensitive power threshold set for CAM i on sub-channel m
$L_{i,m}$	Brief notation of $L(\hat{d}_i, f_m)^{-1}$
$h(L_{i,m})$	Probability distribution of $L_{i,m}$
$\mathcal{H}$	Probability distribution family $h(L_{i,m})$ belongs to
$\sup[\cdot]$, $\inf[\cdot]$	Least upper bound, greatest lower bound
$\mathbb{E}(\cdot)$	The expectation

Consider the link from CAM i to j on sub-channel m with the distance d_{ij}. Since the bandwidth Δf_m in UACs is generally narrow, according to Eqn. (1) and Eqn. (5), we can achieve the link capacity as

$$c_{ij}^m = \Delta f_m \cdot \log_2\left(1 + \frac{p_i^m \cdot L\left(d_{ij}, f_m\right)^{-1}}{N(f_m) \cdot \Delta f_m}\right). \tag{7}$$

C. Modeling of Dolphin Activities

Cetacean biologists have pointed out that dolphins' activities have close relationship with the physical environment, including depth, temperature, currents, tides, chlorophyll concentration, etc. [23]. Considering CAM $i \in \mathcal{N}$, since it is fixed on the ocean floor, the surrounding physical environment is relatively stable, which corresponds to specific characteristics of dolphins' activities, i.e., in some areas nearby some CAMs, dolphins are highly active, but in some other areas, they barely appear. To capture the characteristics of dolphins' activities nearby CAM $i \in \mathcal{N}$, we leverage a parameter $\hat{d}_i$ representing the distance between CAM i and the nearest dolphin group away from it, and we define this parameter as the *dolphin-active distance* of CAM i.

For the dolphin-active distance of CAM $i \in \mathcal{N}$, it can be regarded as a random variable with certain probability distribution relying on surrounding physical environmental features. The specific probability distribution of this distance corresponding to CAM i might be hardly obtained, but the expectation, i.e., the average dolphin-active distance, denoted as $\mathbb{E}(\hat{d}_i)$, can be achieved approximatively by sampling statistics. To be specific, as in [23] where 82 acoustic recorders were deployed on the west Florida shelf to investigate the dolphins' distribution, the dolphin-active distance can be measured by deploying some acoustic recorders nearby the CAMs. Different acoustic recorders are away from different CAMs with different distances, and each one detects the sound of dolphins within its surrounding area regularly. Then, a series of data can be obtained and the statistic characteristic can be achieved by analyzing the recorded samples.[3] Intuitively, for CAM $i \in \mathcal{N}$, the more active surrounding dolphins are, the shorter average dolphin-active distance is and the lower transmission power CAM i should adopt. Some frequently used notations are listed in Table I.

III. DOLPHIN-AWARE MULTI-HOP DATA TRANSMISSION

Since CAMs are anchored to the floor of the ocean, the SS is supposed to know the deployed locations of all CAMs in advance. Then, the location-based statistical characteristics of dolphins' activities nearby each CAM can be captured. Furthermore, the distance-frequency-based capacity of different links can be obtained by the SS as well. Then, the SS can

[3] Actually, passive acoustic monitoring is increasingly being used in cetacean research to effectively monitor the distribution and activity patterns of cetaceans [34]. Biologists are usually willing to collect or have collected such cetacean activity data for their research, which could be used as the priori knowledge to guide the environmental friendly underwater data transmission.

utilize these information to design an optimal data transmission scheme with controllable impact on dolphins.[4]

Considering the M sub-channels, for CAM i, $\forall i \in \mathcal{N}$, with a full transmission power $P_i^{\max}$, there are M maximal transmission ranges correspondingly which are denoted as $R_{i,m}^{\mathrm{Tmax}}$, $m = 1, \cdots, M$. We define the set of CAMs located within the maximal transmission range corresponding to sub-channel m of CAM i as its *m-th transmission neighbor set* denoted as

$$\mathcal{T}_i^m = \left\{ j | d_{ij} \le R_{i,m}^{\mathrm{Tmax}}, j \ne i, m \in \mathcal{M} \right\}. \tag{8}$$

Then, all transmission neighbors of CAM i are $\mathcal{T}_i = \mathcal{T}_i^1 \cup \mathcal{T}_i^2 \cdots \cup \mathcal{T}_i^M$.

Similarly, we denote the M maximal interference ranges of CAM k, $\forall k \in \mathcal{N}$, as $R_{k,m}^{\mathrm{Imax}}$, $m = 1, \cdots, M$, which can be calculated based on Eqn. (4). Then we define the set of CAMs which may interfere with CAM j on sub-channel m as its *m-th interference neighbor set* expressed as

$$I_j^m = \left\{ k | d_{kj} \le R_{k,m}^{\mathrm{Imax}}, k \ne j, m \in \mathcal{M}, \mathcal{T}_k^m \ne \emptyset \right\}. \tag{9}$$

Based on these notations, next, we will present interference constraints, flow routing constraints, and transmission power constraints for the dolphin-aware multi-hop data transmission.

A. Interference Constraints

Considering the link from CAM i to CAM j, $\forall i \ne j \in \mathcal{N}$, we exploit a binary value to describe the condition of the link on sub-channel m, $\forall m \in \mathcal{M}$, as

$$x_{ij}^m = \begin{cases} 1, & \text{if link } i \text{ to } j \text{ uses sub-channel } m, \\ 0, & \text{otherwise.} \end{cases} \tag{10}$$

Firstly, for CAM $i \in \mathcal{N}$, it cannot transmit to or receive from multiple CAMs on the same sub-channel. Therefore, we have[5]

$$\text{I1: } \sum_{j \in \mathcal{T}_i^m} x_{ij}^m \le 1 \quad \text{and} \quad \sum_{\{t | i \in \mathcal{T}_t^m\}} x_{ti}^m \le 1. \tag{11}$$

Besides, one sub-channel cannot be used for transmitting and receiving simultaneously at CAM $j \in \mathcal{N}$, due to the "self-interference" at physical layer. Thus, we have

$$\text{I2: } x_{ij}^m + \sum_{q \in \mathcal{T}_j^m} x_{jq}^m \le 1, \quad \forall i \in \mathcal{N}, \ j \in \mathcal{T}_i^m. \tag{12}$$

Furthermore, interference among different CAMs should be taken into account as well. Note that if CAM $j \in \mathcal{N}$ is receiving data on sub-channel $m \in \mathcal{M}$, any other CAMs, which can cause interference to it, cannot work on the same sub-channel m simultaneously. Therefore, based on Eqn. (9), it can be written as[6]

$$\text{I3: } x_{ij}^m + \sum_{l \in \mathcal{T}_k^m} x_{kl}^m \le 1, \quad \forall i \in \mathcal{N}, \ j \in \mathcal{T}_i^m, \ k \in I_j^m, \ k \ne i. \tag{13}$$

B. Flow Routing Constraints

Beyond the interference management, flow routing has important impact on end-to-end throughput as well. Let f_{ij} denote the flow arranged on the link from CAM i to CAM j, $\forall i \ne j \in \mathcal{N}$. The flow balance equations are presented as follows.

Firstly, considering the source CAM s, the total incoming data should be zero, which can be denoted as

$$\text{F1: } \sum_{\{j | s \in \mathcal{T}_j\}} f_{js} = 0. \tag{14}$$

On the contrary, for the destination CAM d, there is no outgoing data. Thus, we can obtain the second constraint as

$$\text{F2: } \sum_{j \in \mathcal{T}_d} f_{dj} = 0. \tag{15}$$

Next, consider an intermediate CAM i, $i \ne s$ and $i \ne d$. The amount of its incoming data should be equal to that of its outgoing data. Hence, the third constraint can be written as

$$\text{F3: } \sum_{\{p | i \in \mathcal{T}_p\}}^{p \ne d} f_{pi} = \sum_{j \in \mathcal{T}_i}^{j \ne s} f_{ij}, \quad i \ne s, \ i \ne d. \tag{16}$$

In addition, for any link from CAM i to CAM j, $\forall i \ne j \in \mathcal{N}$, if it is active under the interference constraints, i.e., $\exists x_{ij}^m = 1$, $m \in \mathcal{M}$, the total flow arranged on it cannot exceed its capacity, which can be expressed as:

$$\text{F4: } f_{ij} \le \sum_{\{m | j \in \mathcal{T}_i^m\}} c_{ij}^m \cdot x_{ij}^m, \tag{17}$$

where c_{ij}^m is the link capacity as indicated in (7).

C. Transmission Power Constraints with Dolphin-awareness

Denote $\hat{p}_{ij}^m$ the transmission power from CAM i to CAM j on sub-channel m, $\forall i \ne j \in \mathcal{N}$, $\sum_{j \in \mathcal{T}_i^m} \hat{p}_{ij}^m = p_i^m$. Obviously, if $x_{ij}^m = 0$, then $\hat{p}_{ij}^m = 0$. Thus, we can obtain that

$$0 \le \hat{p}_{ij}^m \le P_i^{\max} \cdot x_{ij}^m. \tag{18}$$

[4]In this paper, we consider a static scenario with a constant network topology and thus develop a centralized scheme which is relatively uncomplicated and able to achieve a global optimum. However, when we face the dynamic scenario, the centralized scheme might not be suitable any more and distributed schemes are necessary. Actually, the awareness of dolphin protection can be embedded in the distributed scheme design as well, where each node adjusts its transmission strategy based on the local information, including the dolphins' activities. Furthermore, owing to the distributed manner, the real-time sensing of dolphins at each node can be employed, which can achieve a more effective protection.

[5]Note that the transmission neighbor set is defined based on the maximal transmission range. Since each CAM may not be able to transmit at its full power on certain sub-channel m with dolphin-awareness, some allocated links may be unavailable. Thus, a transmission power constraint to guarantee the successful transmission is needed, which will be shown later.

[6]Note that some interference neighbors of CAM j may not cause interference if they do not apply the full power for transmission. As a result, the constraint I3 may lead to a suboptimal solution. Thus, we will reformulate this interference constraint as a power constraint shown in Section III-C.

Furthermore, if $x_{ij}^m = 1$, to guarantee the successful transmission, the transmission power, $\hat{p}_{ij}^m$, should satisfy that $\hat{p}_{ij}^m \cdot L\left(d_{ij}, f_m\right)^{-1} \geq P_{\mathrm{CAM}}^{\mathrm{T}}$. Mathematically, considering Eqn. (18), the power constraint on $\hat{p}_{ij}^m$ can be expressed as

$$\text{P1:}\quad P_{\mathrm{CAM}}^{\mathrm{T}} \cdot L\left(d_{ij}, f_m\right) \cdot x_{ij}^m \leq \hat{p}_{ij}^m \leq P_i^{\max} \cdot x_{ij}^m. \quad (19)$$

Accordingly, the constraint F4 can be rewritten using $\hat{p}_{ij}^m$ as

$$\text{F4:}\ f_{ij} \leq \sum_{\{m|j\in\mathcal{T}_i^m\}} \Delta f_m \cdot \log_2\left(1 + \frac{\hat{p}_{ij}^m \cdot L\left(d_{ij}, f_m\right)^{-1}}{N\left(f_m\right)\cdot \Delta f_m}\right). \quad (20)$$

Besides the transmission features, next, we will show the power constraint derived from dolphin-awareness. The frequency range used by dolphins for their daily communications is highly overlapped with that used by human underwater acoustic communications. Therefore, it is important to take these 'primary users' into consideration when we design the underwater data transmission scheme, otherwise, those lovely marine animals may suffer bitter experiences or even be killed due to the serious human interference. As a result, we employ a power control strategy to achieve the dolphin-awareness. Based on the patterns of dolphins' activities, which can be captured by field tests and summarized statistically [23], the SS should control the transmission power of the CAMs within or near the dolphin-active areas, or even shut them down and choose other paths for the multi-hop data transmission.

Mathematically, to model the dolphins' activities, we have defined a parameter called dolphin-active distance, $\hat{d}_i$, for CAM $i \in \mathcal{N}$. To protect dolphins, we set M dolphin-sensitive power thresholds corresponding to the M sub-channels for CAM i, which is denoted as $P_{\mathrm{Dol}}^{i,m}$, $m = 1, \cdots, M$. Towards sub-channel $m \in \mathcal{M}$, if CAM i transmits data on it, the interference power caused by it to its nearest dolphin group cannot be higher than the threshold $P_{\mathrm{Dol}}^{i,m}$, which can be expressed as

$$\left(\sum_{j\in\mathcal{T}_i^m} \hat{p}_{ij}^m\right) \cdot L\left(\hat{d}_i, f_m\right)^{-1} \leq P_{\mathrm{Dol}}^{i,m}. \quad (21)$$

The setting of the interference threshold should be closely related with the dolphins' hearing sensitivity. A dolphin's hearing threshold depends on several factors, such as its species, age, sound frequency, gender, etc [35], [36]. General speaking, for relatively low frequencies (e.g. <70 kHz), it usually ranges from 40 to 70 dB re μPa. For example, a 9-year-old bottlenose dolphin yields a hearing threshold as 42 dB re μPa at 60 kHz [37]. An old and an infant Rissos dolphin has a hearing threshold as 63.7, 63.8, 66.5 and 68.8, 71.5, 50.9 dB re μPa at 8, 16, 32 kHz, respectively [36]. Therefore, different dolphin-sensitive thresholds can be set according to different situations and protection levels.

According to Eqn. (21), we can find that for CAM i, $\forall i \in \mathcal{N}$, the smaller $\hat{d}_i$ is (dolphins are active around it), the lower transmission power level should be adopted. Considering that the factor $\hat{d}_i$ is actually a random variable satisfying certain probability distribution, as in [38], we leverage a parameter α to represent a confidence level and have the following dolphin-aware probabilistic power constraint as

$$\text{P2: Pr}\left\{\left(\sum_{j\in\mathcal{T}_i^m} \hat{p}_{ij}^m\right) \cdot L\left(\hat{d}_i, f_m\right)^{-1} \leq P_{\mathrm{Dol}}^{i,m}\right\} \geq \alpha. \quad (22)$$

In addition, consider the link from CAM i to j. If $x_{ij}^m = 1$, then the transmission power of CAM k belonging to the m-th interference neighbor set of CAM j, i.e., $\forall k \in I_j^m$, should be constrained to avoid causing interference, which can be described as

$$\text{P3:}\ \hat{p}_{kl}^m \leq P_k^{\max} - \left(P_k^{\max} - P_{\mathrm{CAM}}^{\mathrm{I}} \cdot L\left(d_{kj}, f_m\right)\right) \cdot x_{ij}^m, \quad (23)$$

where $P_k^{\max}$ is the full power of CAM k and $l \in \mathcal{T}_k^m$. Note that owing to the power constraint P3, all interference neighbors of CAM j will not interfere with it when $x_{ij}^m = 1$, and thus the interference constraint I3 can be covered and deleted. Furthermore, consider any CAM $\hat{k}$ that $j \in \mathcal{T}_{\hat{k}}^m$. Let $k = \hat{k}$ and $l = j$ in Eqn. (23) and we can get $p_{\hat{k}j}^m \leq P_{\mathrm{CAM}}^{\mathrm{I}} \cdot L(d_{\hat{k}j}, f_m)$ if $x_{ij}^m = 1$. Then, based on the constraint P1, we can derive that $x_{\hat{k}j}^m = 0$ because $P_{\mathrm{CAM}}^{\mathrm{T}} > P_{\mathrm{CAM}}^{\mathrm{I}}$. Accordingly, the second term of constraint I1 has been embedded in P1 and P3 as well and thus can also be ignored.

Finally, note that there is also a maximum transmission power constraint, i.e.,

$$\text{P4:}\ \sum_{m\in\mathcal{M}} \sum_{j\in\mathcal{T}_i^m} \hat{p}_{ij}^m \leq P_i^{\max}. \quad (24)$$

D. DAD-Tx Optimization

In this subsection, we formulate the DAD-Tx optimization problem under the aforementioned constraints in terms of interference management, flow routing and power control. To maximize the end-to-end throughput, we adopt the overall flow received at the destination CAM as the objective function. Therefore, the DAD-Tx scheme can be formulated into the probabilistic-constrained optimization problem as shown in the next page, where x_{ij}^m, $\hat{p}_{ij}^m$ and f_{ij} are optimization variables.[7]

IV. Safe Tractable Approximation for Dolphin-Aware Probabilistic Power Constraint

The dolphin-aware probabilistic power constraint, P2, for the DAD-Tx optimization is actually an intractable ambiguous probabilistic constraint because we cannot get the exact probability distribution of $\hat{d}_i$ for each CAM $i \in \mathcal{N}$. Fortunately, the expectation of $\hat{d}_i$, $\mathbb{E}(\hat{d}_i)$, can be obtained approximatively through sampling statistics [23]. Consider that for certain sub-channel $m \in \mathcal{M}$, $L(\hat{d}_i, f_m)^{-1}$ is a function of $\hat{d}_i$. Denote $L(\hat{d}_i, f_m)^{-1}$ as $L_{i,m}$. Then based on sampling statistics, it can also lead to the expectation of $L(\hat{d}_i, f_m)^{-1}$ as $\mathbb{E}\left(L_{i,m}\right)$,

[7] If we only focus on the network performance without dolphin-awareness, the same optimization problem can be formulated without the dolphin-aware power constraint P2, and we call it optimal transmission (Op-Tx) scheme.

DAD-Tx: Maximize $\sum_{\{i|d\in\mathcal{T}_i\}} f_{id}$

s.t. (11), (12), (14), (15), (16), (19), (20), (22), (23), (24)

$x_{ij}^m \in \{0,1\}$ $(i\in\mathcal{N}, j\in\mathcal{T}_i^m, m\in\mathcal{M})$, $f_{ij}\geq 0$ $(i\in\mathcal{N}, i\neq d, j\in\mathcal{T}_i, j\neq s)$, $\hat{p}_{ij}^m \geq 0$ $(i\in\mathcal{N}, j\in\mathcal{T}_i^m, m\in\mathcal{M})$

$$\inf_{t>0}\left[-P_{\mathrm{Dol}}^{i,m}+t^{-1}\cdot\ln\left(\mathbb{E}\left(\exp\left\{t\cdot\left(\sum_{j\in\mathcal{T}_i^m}\hat{p}_{ij}^m\right)\cdot L_{i,m}\right\}\right)\right)-t^{-1}\cdot\ln(1-\alpha)\right]\leq 0. \tag{29}$$

the maximum as $L_{i,m}^{\max}$ and the minimum as $L_{i,m}^{\min}$ approximatively. Therefore, in this section, by using these probabilistic characteristics, we build a tractable conservative approximation of the ambiguous probabilistic constraint P2 [25] using Bernstein approximation to convert P2 into a linear deterministic form.

Recall the probabilistic constraint P2 as

$$\Pr\left\{\left(\sum_{j\in\mathcal{T}_i^m}\hat{p}_{ij}^m\right)\cdot L_{i,m} > P_{\mathrm{Dol}}^{i,m}\right\}\leq 1-\alpha. \tag{25}$$

Let $\xi_i^m=\sum_{j\in\mathcal{T}_i^m}\hat{p}_{ij}^m$ and $\beta=1-\alpha$. Then based on Markov's inequality, we can have

$$\begin{aligned} g\left(L_{i,m}\right) &= \Pr\left\{\xi_i^m\cdot L_{i,m} > P_{\mathrm{Dol}}^{i,m}\right\} \\ &\leq \mathbb{E}\left(\exp\left\{t\cdot\xi_i^m\cdot L_{i,m}\right\}\right)\cdot\exp\left\{-t\cdot P_{\mathrm{Dol}}^{i,m}\right\},\quad t>0, \end{aligned} \tag{26}$$

and derive the following inequality accordingly as

$$\ln\left(g\left(L_{i,m}\right)\right)\leq -t\cdot P_{\mathrm{Dol}}^{i,m}+\ln\left(\mathbb{E}\left(\exp\left\{t\cdot\xi_i^m\cdot L_{i,m}\right\}\right)\right). \tag{27}$$

Consequently, based on Eqn. (27), we can find that for every $\beta\in(0,1)$, if there exists $t>0$ such that

$$-t\cdot P_{\mathrm{Dol}}^{i,m}+\ln\left(\mathbb{E}\left(\exp\left\{t\cdot\xi_i^m\cdot L_{i,m}\right\}\right)\right)\leq\ln(\beta),$$

then $g\left(L_{i,m}\right)\leq\beta$ can be achieved. Mathematically, it can be expressed as

$$\begin{aligned} &\text{if } \exists t>0: \\ &-P_{\mathrm{Dol}}^{i,m}+t^{-1}\cdot\ln\left(\mathbb{E}\left(\exp\left\{t\cdot\xi_i^m\cdot L_{i,m}\right\}\right)\right)-t^{-1}\cdot\ln(\beta)\leq 0 \\ &\text{then}: \ g\left(L_{i,m}\right)\leq\beta. \end{aligned} \tag{28}$$

Thus, we can derive the convex conservative approximation of the probabilistic constraint P2 as (29), as shown at the top of this page.

As it was mentioned, the exact knowledge of the probability distribution of $L_{i,m}$, $h(L_{i,m})$, is unavailable, and we only have its expectation, maximum and minimum. Thus the approximation as Eqn. (29) is still intractable because the value of $\mathbb{E}\left(\exp\left\{t\cdot\xi_i^m\cdot L_{i,m}\right\}\right)$ is hardly derived. Therefore, we adopt a minimax approach to get its tractable conservative approximation, also known as Bernstein approximation. Assume that the distribution $h(L_{i,m})$ belongs to a certain family $\mathcal{H}$. Then, we relax Eqn. (25) as

$$\Pr_{h(L_{i,m})}\left\{\xi_i^m\cdot L_{i,m} > P_{\mathrm{Dol}}^{i,m}\right\}\leq 1-\alpha,\quad \forall h(L_{i,m})\in\mathcal{H}, \tag{30}$$

which can also be expressed as

$$\begin{aligned} &\hat{g}\left(L_{i,m}\right) \\ &\quad=\sup_{h(L_{i,m})\in\mathcal{H}}\left[\Pr_{h(L_{i,m})}\left\{\xi_i^m\cdot L_{i,m} > P_{\mathrm{Dol}}^{i,m}\right\}\right]\leq 1-\alpha. \end{aligned} \tag{31}$$

Let $\Theta\left(L_{i,m}\right)=\max_{h(L_{i,m})\in\mathcal{H}}\ln\left(\mathbb{E}\left(\exp\left\{t\cdot\xi_i^m\cdot L_{i,m}\right\}\right)\right)$. Then similar to Eqn. (27) and Eqn. (28), we can get the following conclusions:

$$\ln\left(\hat{g}\left(L_{i,m}\right)\right)\leq -t\cdot P_{\mathrm{Dol}}^{i,m}+\Theta\left(L_{i,m}\right),\quad t>0, \tag{32}$$

and

$$\begin{aligned} &\text{if } \exists t>0: -P_{\mathrm{Dol}}^{i,m}+t^{-1}\cdot\Theta\left(L_{i,m}\right)-t^{-1}\cdot\ln(\beta)\leq 0 \\ &\text{then}: \ \hat{g}\left(L_{i,m}\right)\leq\beta, \end{aligned} \tag{33}$$

Therefore, similar to Eqn. (29), we obtain the conservative approximation of the ambiguous probabilistic constraint as

$$\inf_{t>0}\left[-P_{\mathrm{Dol}}^{i,m}+t^{-1}\cdot\Theta\left(L_{i,m}\right)-t^{-1}\cdot\ln(\beta)\right]\leq 0. \tag{34}$$

Next, we further derive the tractable conservative approximation of Eqn. (34) based on the expectation, maximum and minimum of $L_{i,m}$. Firstly, we present two lemmas as follows.

Lemma 1: Consider a random variable $x\in[-1,1]$ with expectation μ. Denote the family that its probability distribution $P(x)$ belongs to as $\mathcal{P}$. Then

$$\max_{P(x)\in\mathcal{P}}\ln\left(\mathbb{E}\left(\exp\left\{t\cdot x\right\}\right)\right)=\ln\left(\cosh(t)+\mu\cdot\sinh(t)\right). \tag{35}$$

Proof: See Appendix A. ∎

Lemma 2: For all real numbers γ and λ,

$$\cosh(\lambda)+\gamma\cdot\sinh(\lambda)\leq\exp\left\{\frac{\lambda^2}{2}+\gamma.\lambda\right\}. \tag{36}$$

Proof: See Appendix B. ∎

Based on Eqn. (34) and the two lemmas, we present the following theorem.

Theorem 1: The tractable conservative approximation of the ambiguous probabilistic constraint P2 is shown as (37), as shown at the top of the next page.

Proof: Let

$$\tilde{L}_{i,m}=\frac{2}{L_{i,m}^{\max}-L_{i,m}^{\min}}\cdot L_{i,m}+\frac{L_{i,m}^{\max}+L_{i,m}^{\min}}{L_{i,m}^{\min}-L_{i,m}^{\max}}=a\cdot L_{i,m}+b,$$

$$\left(\sum_{j\in\mathcal{T}_i^m}\hat{p}_{ij}^m\right)\cdot\left(\mathbb{E}\left(L_{i,m}\right)+\sqrt{\frac{\left(L_{i,m}^{\max}-L_{i,m}^{\min}\right)^2}{2}\cdot\ln\left(\frac{1}{1-\alpha}\right)}\right)\le P_{\mathrm{Dol}}^{i,m}. \tag{37}$$

and it is obviously that $\tilde{L}_{i,m}\in[-1,1]$. Recall the conservative approximation Eqn. (34). We have

$$\begin{aligned}&\Theta\left(L_{i,m}\right)\\&=-\frac{t\cdot\xi_i^m\cdot b}{a}+\max_{h\left(L_{i,m}\right)\in\mathcal{H}}\ln\left(\mathbb{E}\left(\exp\left\{\frac{t\cdot\xi_i^m\cdot\tilde{L}_{i,m}}{a}\right\}\right)\right).\end{aligned} \tag{38}$$

Denote $\mathbb{E}\left(\tilde{L}_{i,m}\right)$ as $\tilde{\mu}_{i,m}$. According to Lemma 1 and Lemma 2, it can be derived that

$$\begin{aligned}&\Theta\left(L_{i,m}\right)\\&=-\frac{t\cdot\xi_i^m\cdot b}{a}+\ln\left(\cosh\left(\frac{t\cdot\xi_i^m}{a}\right)+\tilde{\mu}_{i,m}\sinh\left(\frac{t\cdot\xi_i^m}{a}\right)\right)\\&\le-\frac{t\cdot\xi_i^m\cdot b}{a}+\frac{t^2\cdot\left(\xi_i^m\right)^2}{2a^2}+\frac{\tilde{\mu}_{i,m}\cdot t\cdot\xi_i^m}{a}.\end{aligned} \tag{39}$$

Substitute Eqn. (39) into Eqn. (34) and thus we can obtain the tractable conservative approximation as

$$\inf_{t>0}\left[-P_{\mathrm{Dol}}^{i,m}+\xi_i^m\cdot\frac{\tilde{\mu}_{i,m}-b}{a}+\frac{t\cdot\left(\xi_i^m\right)^2}{2a^2}+t^{-1}\cdot\ln\left(\frac{1}{\beta}\right)\right]\le 0. \tag{40}$$

Considering that $\dfrac{\tilde{\mu}_{i,m}-b}{a}=\mathbb{E}\left(L_{i,m}\right)$, Eqn. (40) can be rewritten as

$$\xi_i^m\cdot\left(\mathbb{E}\left(L_{i,m}\right)+\sqrt{\frac{2}{a^2}\cdot\ln\left(\frac{1}{\beta}\right)}\right)\le P_{\mathrm{Dol}}^m. \tag{41}$$

Substituting $\xi_i^m=\sum_{j\in\mathcal{T}_i^m}\hat{p}_{ij}^m$, $a=\dfrac{2}{L_{i,m}^{\max}-L_{i,m}^{\min}}$ and $\beta=1-\alpha$ into Eqn. (41), the conclusion can be achieved. ■

Remark: Note that the Bernstein approximation of P2 as Eqn. (37) actually compresses the solution space and can only lead to a feasible suboptimal solution to the original problem. It is hardly to get the exact loss caused by the approximation because the exact probability distribution of the variable is unavailable. Without loss of generality, we briefly present the approximation ratio for two well-known distributions here, uniform and Gaussian distribution, and for more detailed analysis of Bernstein approximation, interested readers could refer to [25].

Towards the uniform distribution within $\left[L_{i,m}^{\min},L_{i,m}^{\max}\right]$, the original probabilistic constraint expressed as Eqn. (25) can be rewritten as

$$\left(\sum_{j\in\mathcal{T}_i^m}\hat{p}_{ij}^m\right)\le\frac{1}{\alpha\cdot L_{i,m}^{\max}+(1-\alpha)\cdot L_{i,m}^{\min}}\cdot P_{\mathrm{Dol}}^{i,m}. \tag{42}$$

Accordingly, we rewrite the Bernstein approximation denoted as Eqn. (37) here as

$$\begin{aligned}&\left(\sum_{j\in\mathcal{T}_i^m}\hat{p}_{ij}^m\right)\\&\le\frac{P_{\mathrm{Dol}}^{i,m}}{\left(\dfrac{L_{i,m}^{\max}+L_{i,m}^{\min}}{2}+\sqrt{\dfrac{\left(L_{i,m}^{\max}-L_{i,m}^{\min}\right)^2}{2}\cdot\ln\left(\dfrac{1}{1-\alpha}\right)}\right)}\\&=\kappa\cdot\frac{1}{\alpha\cdot L_{i,m}^{\max}+(1-\alpha)\cdot L_{i,m}^{\min}}\cdot P_{\mathrm{Dol}}^{i,m},\end{aligned} \tag{43}$$

where κ is the approximation ratio representing the loss level caused by the Bernstein approximation. Then, we can achieve that

$$\kappa=\frac{\alpha\cdot L_{i,m}^{\max}+(1-\alpha)\cdot L_{i,m}^{\min}}{\left(\dfrac{L_{i,m}^{\max}+L_{i,m}^{\min}}{2}+\sqrt{\dfrac{\left(L_{i,m}^{\max}-L_{i,m}^{\min}\right)^2}{2}\cdot\ln\left(\dfrac{1}{1-\alpha}\right)}\right)}. \tag{44}$$

Next, consider the Gaussian distribution with expectation μ and variance σ^2. We treat the upper bound as $L_{i,m}^{\max}=\mu+3\sigma$ and the lower bound as $L_{i,m}^{\min}=\mu-3\sigma$. Then the original probabilistic constraint can be rewritten as

$$\Pr\left\{L_{i,m}<\frac{P_{\mathrm{Dol}}^{i,m}}{\xi_i^m}\right\}\ge\alpha\Rightarrow\phi\left(\frac{\frac{P_{\mathrm{Dol}}^{i,m}}{\xi_i^m}-\mu}{\sigma}\right)\ge\alpha, \tag{45}$$

in which $\xi_i^m=\sum_{j\in\mathcal{T}_i^m}\hat{p}_{ij}^m$ and $\phi(\cdot)$ is the cumulative distribution function of the normal distribution. According to the normal distribution chart (ϕ-function chart), considering a given α, similar to the derivation of Eqn. (42), we can get the constraint on ξ_i^m as well. For example, let $\alpha=0.8$. Then based on Eqn. (45), we can obtain that

$$\frac{\frac{P_{\mathrm{Dol}}^{i,m}}{\xi_i^m}-\mu}{\sigma}\ge 0.85\Rightarrow\xi_i^m\le\frac{1}{0.85\sigma+\mu}\cdot P_{\mathrm{Dol}}^{i,m}, \tag{46}$$

and the approximation ratio can be derived accordingly as

$$\kappa=\frac{\mu+0.85\sigma}{\mu+5.4\sigma}. \tag{47}$$

Replacing the intractable ambiguous probabilistic constraint P2 by its tractable conservative approximation Eqn. (37), we can find that the DAD-Tx optimization problem is in the form of *mixed-integer non-linear program* (MINLP), which

is NP-hard in general [39]. Therefore, in the next section, we develop a three-phase solution procedure, which can yield a heuristic solution.

V. Three-Phase Solution Procedure

A. Overview

Observing the original MINLP DAD-Tx optimization problem, we find that the difficulty to solve this problem mainly comes from two parts. One is the non-linear part, i.e., the nonpolynomial terms in constraint F4 (log-function), and the other one is about the integer variables x_{ij}^m. Therefore, as the first phase, we construct a convex hull for each nonpolynomial term and relax the non-linear constraint into several linear constraints. Then, the original problem is converted into a relaxed mixed-integer linear program (R-MILP) problem. Based on it, we propose a heuristic algorithm to determine all integer variables x_{ij}^m by solving sequential LP problems iteratively. Once the integer variables are fixed, the R-MILP problem then turns to be a R-LP problem and other variables $\hat{p}_{ij}^m$ and f_{ij} can be derived accordingly.

Nevertheless, the values of f_{ij}-variables attained by solving this R-LP problem may not be feasible due to the linear relaxation of the link capacity. Therefore, we further add a step to re-calculate the values of f_{ij}-variables for feasible solutions. To be specific, we substitute the determined $\hat{p}_{ij}^m$-variables and x_{ij}^m-variables into the original MINLP problem and thus can get a LP problem. Then, the feasible values of f_{ij}-variables can be obtained by solving this LP problem. As a result, after the three phases, we can get a heuristic solution, which is actually a suboptimal solution and can be regarded as a lower bound of the original MINLP problem.

B. Phase 1: Convex Hull Based Linear Relaxation

From the original MINLP problem, we can find that the non-linear part only comes from the constraint F4 as Eqn. (20). Therefore, as the first phase, we relax each nonpolynomial term (log-function) in constraint F4 based on its convex hull and convert it into several linear constraints. Specifically, we introduce a new variable v_{ij}^m for each nonpolynomial term as

$$v_{ij}^m = \log_2\left(1 + \frac{\hat{p}_{ij}^m \cdot L\left(d_{ij}, f_m\right)^{-1}}{N\left(f_m\right) \cdot \Delta f_m}\right), \quad \forall i \in \mathcal{N}, \ j \in \mathcal{T}_i^m. \tag{48}$$

For simplicity, we rewrite it as

$$v_{ij}^m = \log_2\left(\gamma_{ij}^m\right). \tag{49}$$

Obviously, according to the power constraints, we can find that $\hat{p}_{ij}^m$ has a lower bound as $\hat{p}_{ij\_l}^m = 0$ and an upper bound as

$$\hat{p}_{ij\_u}^m = \min\left[P_{\mathrm{Dol}}^{i,m} \cdot \left(\mathbb{E}\left(L_{i,m}\right) + \sqrt{\frac{2}{a^2} \cdot \ln\left(\frac{1}{1-\alpha}\right)}\right)^{-1}, P_i^{\max}\right],$$

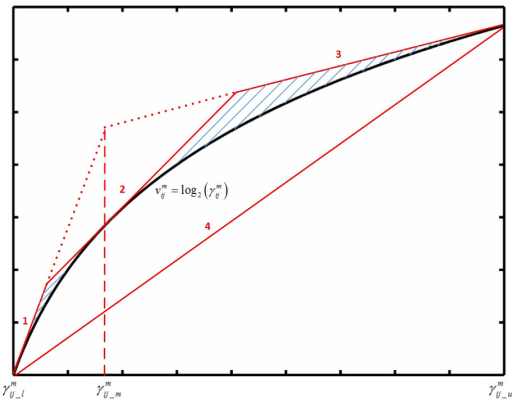

Fig. 2. Linear relaxation based on convex hull with 3 tangents.

where $a = \dfrac{2}{L_{i,m}^{\max} - L_{i,m}^{\min}}$. Note that for certain link CAM i to CAM j on sub-channel m,

$$\frac{L\left(d_{ij}, f_m\right)^{-1}}{N\left(f_m\right) \cdot \Delta f_m} = \eta_{ij}^m$$

is a constant, and thus we can obtain that γ_{ij}^m exists a lower bound denoted as $\gamma_{ij\_l}^m$, and an upper bound denoted as $\gamma_{ij\_u}^m$, which can be calculated as

$$\gamma_{ij\_l}^m = 1 \le \gamma_{ij}^m \le 1 + \hat{p}_{ij\_u}^m \cdot \eta_{ij}^m = \gamma_{ij\_u}^m. \tag{50}$$

Then, based on the bounds of γ_{ij}^m as shown in Eqn. (50), we can construct a convex hull for the function as Eqn. (49), which is composed by n segments ($n-1$ of them are tangential supports and one is the chord). In our paper, we take $n = 4$ as shown in Fig. 2. To be specific, the three tangential segments are at $(\gamma_{ij\_l}^m, \log_2(\gamma_{ij\_l}^m))$, $(\gamma_{ij\_m}^m, \log_2(\gamma_{ij\_m}^m))$, and $(\gamma_{ij\_u}^m, \log_2(\gamma_{ij\_u}^m))$, where $\gamma_{ij\_m}^m$ is the horizontal axis of the intersection of the other two tangents as

$$\gamma_{ij\_m}^m = \frac{\gamma_{ij\_l}^m \cdot \gamma_{ij\_u}^m \cdot \left(\log_2(\gamma_{ij\_u}^m) - \log_2(\gamma_{ij\_l}^m)\right)}{\gamma_{ij\_u}^m - \gamma_{ij\_l}^m} \cdot \ln 2.$$

Since the log-function is within the region of the convex hull, the convex hull based constraints for each v_{ij}^m are four linear constraints, which can be expressed as (51), as shown at the bottom of the next page.

Remark: Note that the objective of the optimization is to maximize the end-to-end throughput, which is limited by v_{ij}^m-variables. Thus the optimal values of v_{ij}^m-variables will be almost surly laid on the upper bound of the convex hull region to achieve the maximal flow rate. Accordingly, instead of using the region as the constraints, we can only use the tangents as the upper bound, i.e., the fourth constraint in (51) can be ignored, and the difference only reflects in the gap between the upper bound and the log-function as shown in Fig. 2. Actually, we could set more points of tangency for the convex hull, rather than three adopted in this paper, to achieve a tighter upper bound as shown in Fig. 3.

As a result, the constraint F4 can be relaxed as

$$f_{ij} \le \sum_{\{m | j \in \mathcal{T}_i^m\}} \Delta f_m \cdot v_{ij}^m, \tag{52}$$

with three additional linear constraints for each v_{ij}^m.

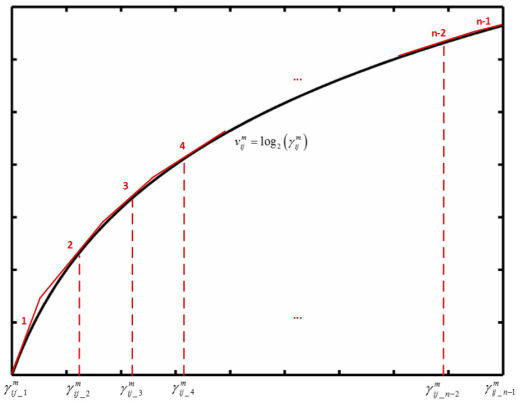

Fig. 3. Linear relaxation based on convex hull with n-1 tangents.

C. Phase 2: Heuristic Relax-and-Fix Based Iterative Algorithm

Through the convex hull based linear relaxation, the original MINLP problem turns to be a relaxed MILP (R-MILP) problem. However, due to the integer variables, this problem is still NP-hard. Therefore, in this subsection, we propose a heuristic relax-and-fix based iterative (HRFI) algorithm to determine all integer variables by solving sequential LP problems iteratively. In the HRFI algorithm, during each iteration, we relax the integer variable as $0 \le x_{ij}^m \le 1$ and get the optimal solution by solving a LP problem. Then we determine some of the integer variables according to certain rules and fix them in the subsequent iterations until all integer variables are determined.

To be specific, in the first iteration, we relax all the integer variables to $0 \le x_{ij}^m \le 1$, $\forall m \in \mathcal{M}$, $\forall i \in \mathcal{N}$, $\forall j \ne i \in \mathcal{I}_i^m$, and the R-MILP problem is converted into a LP problem. Through solving the LP problem, we can obtain an optimal solution with relaxed integer variables. Among them, we select the maximal one $x_{i^*j^*}^{m^*}$ and set it to 1. Observing all power constraints, on one hand, if there is no contradiction with $x_{i^*j^*}^{m^*} = 1$, then we fix it as $x_{i^*j^*}^{m^*} = 1$. After that, according to the interference constraints I1 and I2, we can determine some other integer variables accordingly. Specifically, based on I1, we can have $x_{i^*j}^{m^*} = 0, \forall j \ne j^* \in \mathcal{I}_{i^*}^{m^*}$ and $x_{ti^*}^{m^*} = 0, \left\{\forall t | i^* \in \mathcal{I}_t^{m^*}\right\}$. From I2, we can get $x_{j^*q}^{m^*} = 0$, $\forall q \in \mathcal{I}_{j^*}^{m^*}$. On the other hand, if there exists contradiction with $x_{i^*j^*}^{m^*} = 1$, then we fix $x_{i^*j^*}^{m^*} = 0$ and continue the iteration.

Next, in the second iteration, we substitute the fixed integer variables into the R-MILP problem, relax the remaining un-fixed integer variables and achieve an updated LP problem. Then we solve the new LP problem and fix some additional integer variables based on the same process. We continue the iteration until fixing all the integer variables.

D. Phase 3: Determining Other Variables

In the first phase, according to the convex hull based linear relaxation, we reformulate the non-linear constraint with log-function in terms of some linear constraints, and thus get a R-MILP problem. Then, towards the R-MILP problem, by using the HRFI algorithm, all integer variables can be fixed. Next, in this subsection, we will determine all other variables and seek for the heuristic solution.

Obviously, by substituting the determined integer variables into the R-MILP problem, we can obtain a R-LP problem, and $\hat{p}_{ij}^m$-variables and f_{ij}-variables can be attained accordingly. Unfortunately, since this LP problem is a relaxed one, in which we use a convex hull region instead of the log-function for link capacity, the obtained values of f_{ij}-variables may not be feasible and exceed the real link capacity. Therefore, to derive the feasible values of f_{ij}-variables, we employ an additional step. To be specific, we fix the values of x_{ij}^m-variables and $\hat{p}_{ij}^m$-variables obtained by solving the R-MILP problem and the R-LP problem respectively, and substitute them into the original MINLP problem. Then, we have a LP problem as follows.

$$
\begin{aligned}
&\text{Maximize} \sum_{j \in \mathcal{I}_s} f_{sj} \\
&\text{s.t.} \sum_{\{j | s \in \mathcal{I}_j^m\}} f_{js} = 0, \sum_{j \in \mathcal{I}_d} f_{dj} = 0, \\
&\sum_{i \in \mathcal{I}_p}^{p \ne d} f_{pi} = \sum_{j \in \mathcal{I}_i}^{j \ne s} f_{ij} \ \ (p \in \mathcal{N}, i \ \ne s, i \ \ne d), \\
&f_{ij} \le \sum_{\{m | j \in \mathcal{I}_i^m\}} \Delta f_m \cdot l\left(\hat{p}_{ij}^m\right), \\
&f_{ij} \ge 0 \ \ (i \in \mathcal{N}, i \ne d, j \in \mathcal{I}_i, j \ne s),
\end{aligned}
$$

where $l\left(\hat{p}_{ij}^m\right)$ is a constant derived by the log-function with the determined $\hat{p}_{ij}^m$-variables. Based on this LP problem, the feasible values of f_{ij}-variables can be determined and thus the heuristic solution is obtained.

$$
\begin{aligned}
\gamma_{ij\_l}^m \cdot \ln 2 \cdot v_{ij}^m &\le \gamma_{ij}^m + \gamma_{ij\_l}^m \cdot \ln 2 \cdot \left(\log_2\left(\gamma_{ij\_l}^m\right) - \frac{1}{\ln 2}\right), \\
\gamma_{ij\_u}^m \cdot \ln 2 \cdot v_{ij}^m &\le \gamma_{ij}^m + \gamma_{ij\_u}^m \cdot \ln 2 \cdot \left(\log_2\left(\gamma_{ij\_u}^m\right) - \frac{1}{\ln 2}\right), \\
\gamma_{ij\_m}^m \cdot \ln 2 \cdot v_{ij}^m &\le \gamma_{ij}^m + \gamma_{ij\_m}^m \cdot \ln 2 \cdot \left(\log_2\left(\gamma_{ij\_m}^m\right) - \frac{1}{\ln 2}\right), \\
\left(\gamma_{ij\_u}^m - \gamma_{ij\_l}^m\right) . v_{ij}^m &\ge \left(\log_2\left(\gamma_{ij\_u}^m\right) - \log_2\left(\gamma_{ij\_l}^m\right)\right) \cdot \gamma_{ij}^m + \gamma_{ij\_u}^m \cdot \log_2\left(\gamma_{ij\_l}^m\right) - \gamma_{ij\_l}^m \cdot \log_2\left(\gamma_{ij\_u}^m\right). \qquad (51)
\end{aligned}
$$

TABLE II
20 DATA SETS OF THE END-TO-END THROUGHPUT (Kbps) BASED ON OP-TX SCHEME AND DAD-TX SCHEME

Index	Op-Tx	DAD-Tx 130 dB	DAD-Tx 120 dB	DAD-Tx 110 dB	Index	Op-Tx	DAD-Tx 130 dB	DAD-Tx 120 dB	DAD-Tx 110 dB
1	96.31	96.31	89.39	0	11	97.54	97.54	91.34	0
2	95.97	95.97	91.52	0	12	91.85	91.85	86.14	0
3	94.29	0	0	0	13	105.03	105.03	105.03	105.03
4	99.11	99.11	61.80	0	14	97.48	97.48	91.84	0
5	116.12	116.12	116.12	116.12	15	121.18	97.65	0	0
6	99.74	99.74	93.33	0	16	94.29	0	0	0
7	104.84	104.84	104.84	92.83	17	104.25	104.25	96.42	0
8	97.46	97.46	97.46	97.46	18	102.26	102.26	97.15	0
9	91.21	91.21	91.21	83.45	19	99.74	99.74	96.34	0
10	96.21	96.21	0	0	20	101.4	0	0	0

VI. PERFORMANCE EVALUATION

A. Simulation Setup

By using empirical data of dolphins' occurrence on the West Florida Shelf (WFS) [23], we consider a MUCAN with $|\mathcal{N}| = 15$ CAMs deployed in a 20×20 km^2 area across three regions (horizontal axis: 0∼5, 5∼15, 15∼20), namely, inner shelf (IS), mid shelf (MS) and outer shelf (OS). Suppose that there are five available sub-channels ranging from 10 kHz to 40 kHz with identical bandwidth as 6 kHz and central frequencies as $\{13, 19, 25, 31, 37\}$ kHz. We take the SM-75 (Smart Modem 75) as the CAM in the MUCAN [40], and the transmission power at each CAM is 190 dB re μPa (corresponding to 6.67W) according to the user's manual. The transmission and interference power threshold is set to 120 and 100 dB re μPa, respectively. Then, refer to Section II-B, we can obtain the transmission and interference range corresponding to the five sub-channels, which are {9.61, 5.73, 3.94, 2.97, 2.38} km and {17.98, 10.06, 6.66, 4.89, 3.84} km, respectively. Towards the noise, we set $s = 0.5$ and $\omega = 2.5$ m/s, and for the transmission loss, we set $k = 1.5$ and omit the constant A as in [30] and [31]. Sufficient data in [23] show the fact that dolphins' activities are influenced by depths significantly. To be specific, the closer area to the coast, the more active dolphins present, i.e., the active level of dolphins follows a decreasing order from IS region to OS region (from [23, Tables 4.1–4.3]). In our simulation, we take 20 samples of dolphin-active distance for each CAM, and $\mathbb{E}(\hat{d}_i)$ and $\mathbb{E}(L_{i,m})$ can be obtained accordingly. Since the higher active level corresponds to the shorter dolphin-active distance, the 20 samples of each CAM located within the IS, MS, and OS region are random variables within $[1, 3]$ km, $[6, 8]$ km, and $[11, 13]$ km, respectively.

B. Results and Analysis

Firstly, we show the end-to-end throughput of the MUCAN based on the proposed DAD-Tx scheme with different levels of dolphin-awareness and the optimal transmission (Op-Tx) scheme without dolphin-awareness as Table II. For the DAD-Tx scheme, we set the dolphin-sensitive power threshold on all sub-channels for all CAMs the same. We consider three levels as 110 dB re μPa, 120 dB re μPa, and 130 dB re μPa,[8] and the confidence level is set as $\alpha = 0.9$. Obviously, a less dolphin-sensitive power threshold corresponds to a higher level of dolphin-awareness. For the Op-Tx scheme, there is no dolphin-sensitive power threshold for each CAM, and the maximal end-to-end throughput can be achieved by solving the same optimization problem as the DAD-Tx scheme but without the dolphin-aware power constraint P2.

We employ 20 data sets corresponding to 20 different network topologies. For each data set, we choose one source CAM and one destination CAM randomly among the 15 CAMs. Comparing different schemes, we can find that the Op-Tx scheme can achieve the best end-to-end throughput, and the less level of dolphin-awareness (higher dolphin-sensitive power threshold) is, the higher end-to-end throughput can be reached. Take the 7th and 9th data set as an example. We can find that in both scenarios, available paths exist for all three levels of dolphin-sensitive power threshold, and the end-to-end throughput under the 110 dB level is the worst. When the threshold is raised to 120 dB and 130 dB, the DAD-Tx scheme can achieve the same end-to-end throughput as the Op-Tx scheme because the CAMs cannot cause interference higher than 120 dB in both scenarios even when they use the full transmission power and thus the dolphin-aware power constraint P2 will have no constraining force. Furthermore, there are also some special cases. As the 3rd, 16th and 20th data set, all involved CAMs are located within the IS region with short dolphin-active distance. Therefore, no path is available even for the high threshold. By contrast, as the 5th, 8th and 13rd data set, all involved CAMs are located within the OS region where dolphins barely appear and thus the DAD-Tx scheme can achieve the maximal end-to-end throughput as the Op-Tx scheme even for the low threshold.

Next, to demonstrate the effectiveness of dolphin-awareness brought by the DAD-Tx scheme, we adopt a one-shot experiment with a random network topology shown as Fig. 4. CAM 13 and CAM 15 are chosen randomly as the source and the destination, respectively. Different CAMs are located within different regions corresponding to different characteristics of dolphins' activities, and we employ a parameter called dolphin-active distance for each CAM to represent the active level of dolphins near it. According to the 20 samples for each CAM (20 random variables within different ranges for the CAMs located within different regions), the mean values of dolphin-active distance are shown as Table III. Dolphins are more likely to appear within IS region but barely appear within

[8]Although such power levels may not kill dolphins immediately, they are about 60 dB higher than dolphins' hearing threshold, which may cause several long-term harmful impacts on them and threaten their populations if they are exposed into such a noisy environment for a long time [13].

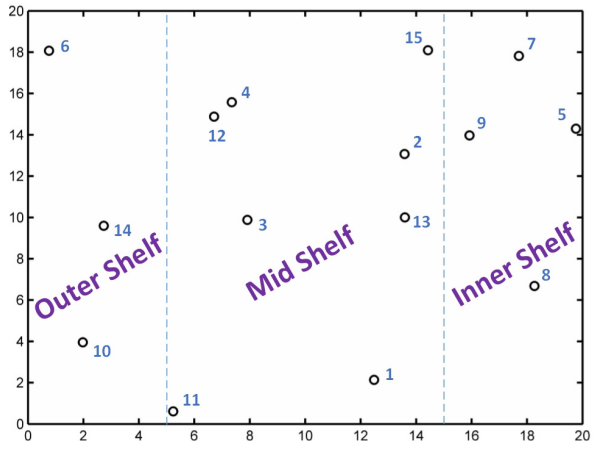

Fig. 4. Multi-hop underwater cognitive acoustic network with 15 CAMs deployed randomly.

TABLE III
AVERAGE DOLPHIN-ACTIVE DISTANCE FOR EACH CAM (KM)

CAM No.	$\mathbb{E}(\hat{d}_i)$	CAM No.	$\mathbb{E}(\hat{d}_i)$	CAM No.	$\mathbb{E}(\hat{d}_i)$
1	6.93	2	7.12	3	7.02
4	7.03	5	1.81	6	12.06
7	2.18	8	2.30	9	2.14
10	11.98	11	6.93	12	7.09
13	6.96	14	11.99	15	6.98

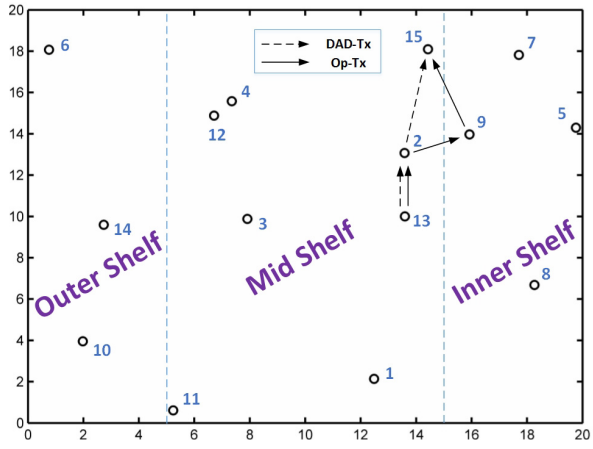

Fig. 5. Strategies for data transmission from CAM 13 to CAM 15 based on Op-Tx scheme and DAD-Tx scheme.

OS region [23]. Accordingly, the CAMs located within IS region have shorter dolphin-active distances and those located within OS region have longer ones.

Then, in this MUCAN, we adopt the two different schemes, i.e., Op-Tx scheme without dolphin-awareness and DAD-Tx scheme, and obtain two different strategies for data transmission from CAM 13 to CAM 15 as shown in Fig. 5. For the DAD-Tx scheme, the dolphin-sensitive power thresholds on all sub-channels for all CAMs are set the same as $P_{\text{Dol}}^{i,m} = 120$ dB re μPa, $\forall i \in \mathcal{N}$, $\forall m \in \mathcal{M}$, and the confidence level for dolphin-aware probabilistic power constraint is set as $\alpha = 0.9$. According to the three-phase procedure, the specific

TABLE IV
SOLUTIONS OF Op-Tx SCHEME AND DAD-Tx SCHEME

x_{ij}^m-variables	Op-Tx	$x_{13,2}^2 = 1,\ x_{2,9}^3 = 1,\ x_{9,15}^1 = 1$
	DAD-Tx	$x_{13,2}^2 = 1,\ x_{2,15}^1 = 1$
$\hat{p}_{ij}^m$-variables	Op-Tx	$\hat{p}_{13,2}^2 = 4.05,\ \hat{p}_{2,9}^3 = 6.67,\ \hat{p}_{9,15}^1 = 6.67$
	DAD-Tx	$\hat{p}_{13,2}^2 = 1.64,\ \hat{p}_{2,15}^1 = 3.37$
throughput	Op-Tx	100.06 kbps
	DAD-Tx	89.54 kbps

solutions of both schemes are shown in Table IV. We can see that when Op-Tx scheme is adopted, the routing path is set to $13 \rightarrow 2 \rightarrow 9 \rightarrow 15$, i.e., the solid line from CAM 13 to CAM 15 in Fig. 5. There is no dolphin-sensitive power threshold on each CAM, and the transmission power and the flow routing is arranged aiming to maximize the end-to-end throughput reaching 100.06 kbps. Nevertheless, when DAD-Tx scheme is utilized, power threshold is adopted to avoid causing serious impact on dolphins. Since the CAM 9 is located within IS region, where dolphins are more active than other regions, the CAM 9 is shut down and a new routing path $13 \rightarrow 2 \rightarrow 15$, i.e., the dotted line, is employed. Accordingly, although the end-to-end throughput is slightly reduced to 89.54 kbps, the new path can achieve dolphin-awareness effectively.

VII. CONCLUSION AND FUTURE WORKS

To realize the environmental friendly transmission in MUCANs, in this paper, we have proposed a DAD-Tx scheme aiming to achieve the optimal end-to-end throughput with dolphin-awareness. Based on statistical features, we have modeled the dolphins' activities and mathematically described the dolphin-awareness as a probabilistic constraint. Then, under dolphin-awareness and multiple wireless acoustic transmission constraints, we have further formulated the DAD-Tx optimization problem. Considering the intractable probabilistic constraint, we have exploited Bernstein approximation approach to convert the formulated problem to a MINLP one, and developed a three-phase procedure for feasible solutions. Through simulations, we show that, in MUCANs, the proposed DAD-Tx scheme can effectively achieve dolphin-awareness and meanwhile reach the optimal end-to-end throughput. As our future works, we will continue to focus on the underwater environmental friendly transmission design, further consider some more complicated scenarios, e.g., dynamic scenarios, and try to develop some more sophisticated schemes, e.g., distributed schemes.

APPENDIX A
PROOF OF LEMMA 1

Proof: Let $f(x) = \exp\{t \cdot x\} - \sinh(t) \cdot x$. Obviously, this function is convex and thus its maximum with $x \in [-1, 1]$ happens at an endpoint, i.e., $f(-1)$ or $f(1)$. Since $f(-1) = f(1) = \cosh(t)$, we have

$$f(x) \leq \cosh(t), \quad x \in [-1, 1]. \tag{53}$$

Furthermore, considering $\mathbb{E}(\exp\{t \cdot x\}) = \int \exp\{t \cdot x\} dP(x)$, according to Eqn. (53), we can obtain

$$\begin{aligned}&\mathbb{E}(\exp\{t \cdot x\}) \\ &= \int f(x)\, dP(x) + \int \sinh(t) \cdot x dP(x) \\ &= \int f(x)\, dP(x) + \mu \cdot \sinh(t) \leq \cosh(t) + \mu \cdot \sinh(t).\end{aligned} \tag{54}$$

Therefore, the conclusion as Eqn. (35) can be obtained. Actually, this upper bound can be achieved when $P(x)$ is a two-point distribution as $P(x) = \frac{1+\mu}{2}$ when $x = 1$ and $P(x) = \frac{1-\mu}{2}$ when $x = -1$. ■

APPENDIX B
PROOF OF LEMMA 2

Proof: Define a function as

$$g(\gamma, \lambda) = \cosh(\lambda) + \gamma \cdot \sinh(\lambda) - \exp\left\{\frac{\lambda^2}{2} + \gamma.\lambda\right\}. \tag{55}$$

Setting its partial derivatives to be zero, we can get

$$\sinh(\lambda) + \gamma \cdot \cosh(\lambda) = (\gamma + \lambda) \cdot \exp\left\{\frac{\lambda^2}{2} + \gamma.\lambda\right\}, \tag{56}$$

and

$$\sinh(\lambda) = \lambda \cdot \exp\left\{\frac{\lambda^2}{2} + \gamma.\lambda\right\}. \tag{57}$$

According to Eqn. (56) and Eqn. (57), we have $\tanh(\lambda) = \lambda$, which means that $\lambda = 0$ corresponds to the extremum. Considering

$$\left.\frac{\partial^2 g(\gamma, \lambda)}{\partial \lambda}\right|_{\lambda=0} = \gamma - \gamma^2 - 1 < 0, \tag{58}$$

and $g(\gamma, 0) = 0$, it can be derived that the maximum of $g(\gamma, \lambda)$ is 0 and thus Eqn. (36) can be achieved. ■

REFERENCES

[1] I. F. Akyildiz, D. Pompili, and T. Melodia, "Underwater acoustic sensor networks: Research challenges," *Ad Hoc Netw.*, vol. 3, no. 3, pp. 257–279, May 2005.

[2] E. M. Sozer, M. Stojanovic, and J. G. Proakis, "Underwater acoustic networks," *IEEE J. Ocean. Eng.*, vol. 25, no. 1, pp. 72–83, Jan. 2000.

[3] J.-H. Cui, J. Kong, M. Gerla, and S. Zhou, "The challenges of building mobile underwater wireless networks for aquatic applications," *IEEE Netw.*, vol. 20, no. 3, pp. 12–18, May 2006.

[4] A. A. Syed, W. Ye, and J. Heidemann, "T-Lohi: A new class of MAC protocols for underwater acoustic sensor networks," in *Proc. IEEE Conf. Comput. Commun. (INFOCOM)*, Phoenix, AZ, USA, Apr. 2008, pp. 231–235.

[5] Z. Guo, B. Wang, P. Xie, W. Zeng, and J.-H. Cui, "Efficient error recovery with network coding in underwater sensor networks," *Ad Hoc Netw.*, vol. 7, no. 4, pp. 791–802, Jun. 2009.

[6] L. Pu *et al.*, "Impact of real modem characteristics on practical underwater MAC design," in *Proc. OCEANS*, Yeosu, South Korea, May 2012, pp. 1–6.

[7] W. J. Richardson, C. R. Greene, Jr., C. I. Malme, and D. H. Thomson, *Marine Mammals and Noise*. San Diego, CA, USA: Academic, 2013.

[8] W. Yonggang, T. Jiansheng, P. Yue, and H. Li, "Underwater communication goes cognitive," in *Proc. OCEANS*, Quebec City, QC, Canada, Sep. 2008, pp. 1–4.

[9] Y. Luo, L. Pu, M. Zuba, Z. Peng, and J.-H. Cui, "Challenges and opportunities of underwater cognitive acoustic networks," *IEEE Trans. Emerg. Topics Comput.*, vol. 2, no. 2, pp. 198–211, Jun. 2014.

[10] Y. Luo, L. Pu, M. Zuba, Z. Peng, and J.-H. Cui, "Cognitive acoustics: Making underwater communications environment-friendly," in *Proc. Int. Conf. Underwater Netw. Syst. (WUWNET)*, Rome, Italy, Nov. 2014, Art. no. 48.

[11] Y. Luo, L. Pu, Z. Peng, Y. Zhu, and J.-H. Cui, "RISM: An efficient spectrum management system for underwater cognitive acoustic networks," in *Proc. IEEE Conf. Sens., Commun., Netw. (SECON)*, Singapore, Jul. 2014, pp. 414–422.

[12] W. Cheng, Y. Luo, Z. Peng, and M. C. Hastings, "A framework of acoustic channel availability prediction for avoiding interfering marine mammals," in *Proc. Int. Conf. Underwater Netw. Syst. (WUWNET)*, Rome, Italy, Nov. 2014, Art. no. 34.

[13] L. S. Weilgart, "A brief review of known effects of noise on marine mammals," *Int. J. Comparative Psychol.*, vol. 20, no. 2, pp. 159–168, 2007.

[14] L. Bejder, "Linking short and longterm effects of naturebased tourism on cetaceans," Ph.D. thesis. Dept. Biology , Dalhousie Univ., Halifax, Canada, Jan. 2005.

[15] *Standard for Cognitive Wireless Regional Area Networks (RAN) for Operation in TV Bands*, IEEE Standard 802.22-2011(TM), Jul. 2011.

[16] I. F. Akyildiz, W.-Y. Lee, M. C. Vuran, and S. Mohanty, "NeXt generation/dynamic spectrum access/cognitive radio wireless networks: A survey," *Comput. Netw.*, vol. 50, no. 4, pp. 2127–2159, Sep. 2006.

[17] L. Ding, K. Gao, T. Melodia, S. N. Batalama, D. A. Pados, and J. D. Matyjas, "All-spectrum cognitive networking through joint distributed channelization and routing," *IEEE Trans. Wireless Commun.*, vol. 12, no. 11, pp. 5394–5405, Nov. 2013.

[18] G. Sklivanitis, E. Demirors, A. M. Gannon, S. N. Batalama, D. A. Pados, and T. Melodia, "All-spectrum cognitive channelization around narrowband and wideband primary stations," in *Proc. IEEE Global Commun. Conf. (GLOBECOM)*, San Diego, CA, USA, Dec. 2015, pp. 1–7.

[19] H. Islam, Y. C. Liang, and A. T. Hoang, "Joint power control and beamforming for cognitive radio networks," *IEEE Trans. Wireless Commun.*, vol. 7, no. 7, pp. 2415–2419, Jul. 2008.

[20] Y. Chen, G. Yu, Z. Zhang, H. H. Chen, and P. Qiu, "On cognitive radio networks with opportunistic power control strategies in fading channels," *IEEE Trans. Wireless Commun.*, vol. 7, no. 7, pp. 2752–2761, Jul. 2008.

[21] G. Sklivanitis, E. Demirors, S. N. Batalama, T. Melodia, and D. A. Pados, "Receiver configuration and testbed development for underwater cognitive channelization," in *Proc. 48th Asilomar Conf. Signals, Syst. Comput.*, Pacific Grove, CA, USA, Nov. 2014, pp. 1594–1598.

[22] E. Demirors, G. Sklivanitis, T. Melodia, S. N. Batalama, and D. A. Pados, "Software-defined underwater acoustic networks: Toward a high-rate real-time reconfigurable modem," *IEEE Commun. Mag.*, vol. 53, no. 11, pp. 64–71, Nov. 2015.

[23] P. Simard, "Dolphin sound production and distribution on the West Florida shelf," M.S. thesis, Dept. Marine Sci., Univ. South Florida, Tampa, FL, USA, Jan. 2012.

[24] M. Pan, P. Li, Y. Song, Y. Fang, P. Lin, and S. Glisic, "When spectrum meets clouds: Optimal session based spectrum trading under spectrum uncertainty," *IEEE J. Sel. Areas Commun.*, vol. 32, no. 3, pp. 615–627, Mar. 2014.

[25] A. Nemirovski and A. Shapiro, "Convex approximations of chance constrained programs," *SIAM J. Optim.*, vol. 17, no. 4, pp. 969–996, Nov. 2006.

[26] P. Casari and A. F. Harris, "Energy-efficient reliable broadcast in underwater acoustic networks," in *Proc. 2nd Workshop Underwater Netw. (WUWNet)*, New York, NY, USA, Sep. 2007, pp. 49–56.

[27] R. Diamant and L. Lampe, "Spatial reuse time-division multiple access for broadcast ad hoc underwater acoustic communication networks," *IEEE J. Ocean. Eng.*, vol. 36, no. 2, pp. 172–185, Apr. 2011.

[28] T. Melodia, H. Kulhandjian, L.-C. Kuo, and E. Demirors, "Advances in underwater acoustic networking," in *Mobile Ad Hoc Networking: Cutting Edge Directions*. Hoboken, NJ, USA: Wiley, 2013, pp. 804–852.

[29] M. Stojanovic, "On the relationship between capacity and distance in an underwater acoustic communication channel," *ACM SIGMOBILE Mobile Comput. Commun. Rev.*, vol. 11, no. 4, pp. 34–43, Oct. 2007.

[30] A. O. Bicen, A. B. Sahin, and O. B. Akan, "Spectrum-aware underwater networks: Cognitive acoustic communications," *IEEE Veh. Technol. Mag.*, vol. 7, no. 2, pp. 34–40, Jun. 2012.

[31] N. Baldo, P. Casari, and M. Zorzi, "Cognitive spectrum access for underwater acoustic communications," in *Proc. IEEE Int. Conf. Commun. Workshops (ICC Workshops)*, Beijing, China, May 2008, pp. 518–523.
[32] Z. Wang, S. Zhou, J. Catipovic, and P. Willett, "Asynchronous multiuser reception for OFDM in underwater acoustic communications," *IEEE Trans. Wireless Commun.*, vol. 12, no. 3, pp. 1050–1061, Mar. 2013.
[33] L. Wan, H. Zhou, D. Wilson, J. Hanson, S. Zhou, and Z. Shi, "Analysis of underwater OFDM performance during a 2-month deployment in Chesapeake bay," *Marine Technol. Soc. J.*, vol. 48, no. 6, pp. 52–64, Dec. 2014.
[34] R. G. Elliott, S. M. Dawson, and S. Henderson, "Acoustic monitoring of habitat use by bottlenose dolphins in doubtful sound, New Zealand," *New Zealand J. Marine Freshwater Res.*, vol. 45, no. 4, pp. 637–649, Jun. 2011.
[35] S. H. Ridgway and D. A. Carder, "Hearing deficits measured in some *Tursiops truncatus*, and discovery of a deaf/mute dolphin," *J. Acoust. Soc. Amer.*, vol. 101, no. 1, pp. 590–594, Jan. 1997.
[36] P. E. Nachtigall, M. M. L. Yuen, T. A. Mooney, and K. A. Taylor, "Hearing measurements from a stranded infant Risso's dolphin, *Grampus griseus*," *J. Experim. Biol.*, vol. 208, no. 21, pp. 4181–4188, Nov. 2005.
[37] C. S. Johnson, "Sound detection thresholds in marine mammals," *Marine Bio-Acoust.*, vol. 2, no. 6, pp. 247–260, 1967.
[38] M. Pan, P. Li, Y. Song, Y. Fang, and P. Lin, "Spectrum clouds: A session based spectrum trading system for multi-hop cognitive radio networks," in *Proc. IEEE Conf. Comput. Commun. (INFOCOM)*, Orlando, FL, USA, Mar. 2012, pp. 1557–1565.
[39] Y. Shi, Y. T. Hou, and H. Zhou, "Per-node based optimal power control for multi-hop cognitive radio networks," *IEEE Trans. Wireless Commun.*, vol. 8, no. 10, pp. 5290–5299, Oct. 2009.
[40] *SM-75 Smart Modem, User's Manual*, Benthos-Inc., North Falmouth, MA, USA, 2005.

Xuanheng Li (S'13) received the B.S. degree in electronic and information engineering from the Dalian University of Technology, Dalian, China, in 2012, where he is currently pursuing the Ph.D. degree in communication and information system. Since 2015, he has been a Visiting Student with the Wireless Networks Laboratory, University of Florida, Gainesville, FL, USA. His research interests include cognitive radio networks, interference management, green communications, and underwater communications. He was a recipient of the Best Paper Award at the IEEE Globecom in 2015. He serves as a Reviewer of the IEEE TRANSACTIONS ON VEHICULAR TECHNOLOGY, the IEEE COMMUNICATIONS LETTERS, the IEEE INTERNET OF THINGS JOURNAL, and the INFOCOM.

Yi Sun (M'06) received the Ph.D. degree in optical engineering from the Dalian University of Technology, Dalian, China, in 2002. From 2006 to 2007, she visited Stanford University as a Senior Visiting Scholar. She is currently a Professor with the School of Information and Communication Engineering, Dalian University of Technology. Her research interests include cognitive radio networks, interference management, green communications, and underwater communications.

Yuanxiong Guo (M'14) received the B.Eng. degree in electronics and information engineering from the Huazhong University of Science and Technology, Wuhan, China, in 2009, and the M.S. and Ph.D. degrees in electrical and computer engineering from the University of Florida, Gainesville, FL, USA, in 2012 and 2014, respectively. Since 2014, he has been an Assistant Professor with the School of Electrical and Computer Engineering, Oklahoma State University, Stillwater, OK, USA. His current research interests include smart grids, data centers, wireless networks, and cyber-physical systems security and privacy. He was a recipient of the Best Paper Award at the IEEE Global Communications Conference in 2011.

Xin Fu received the Ph.D. degree in computer engineering from the University of Florida, Gainesville, FL, USA, in 2009. She is currently an Assistant Professor with the Electrical and Computer Engineering Department, University of Houston, Houston, TX, USA. Her research interests include computer architecture, high-performance computing, hardware reliability and variability, energy-efficient computing, and mobile computing.

Miao Pan (S'07–M'12) received the B.Sc. degree in electrical engineering from the Dalian University of Technology, China, in 2004, the M.A.Sc. degree in electrical and computer engineering from the Beijing University of Posts and Telecommunications, China, in 2007, and the Ph.D. degree in electrical and computer engineering from the University of Florida in 2012, respectively. He was an Assistant Professor in computer science with Texas Southern University from 2012 to 2015. He is currently an Assistant Professor with the Department of Electrical and Computer Engineering, University of Houston, Houston, TX, USA. His research interests include cognitive radio networks, cybersecurity, and cyber-physical systems. His work on cognitive radio network received the Best Paper Award at Globecom 2015. He is currently an Associate Editor of the IEEE INTERNET OF THINGS JOURNAL.